Journal Pre-proof

A highly sensitive endoplasmic reticulum-targeting fluorescent probe for the imaging of endogenous H2S in live cells

Lei Zhou, Zhi-Qiang Cheng, Ning Li, Yong-Xi Ge, Hong-Xu Xie, Kongkai Zhu, Aiqin Zhou, Juan Zhang, Kai-Ming Wang, Cheng-Shi Jiang

PII: S1386-1425(20)30557-6

DOI: https://doi.org/10.1016/j.saa.2020.118578

Reference: SAA 118578

To appear in: *Spectrochimica Acta Part A: Molecular and Biomolecular Spectroscopy*

Received date: 28 April 2020

Revised date: 30 May 2020

Accepted date: 1 June 2020

Please cite this article as: L. Zhou, Z.-Q. Cheng, N. Li, et al., A highly sensitive endoplasmic reticulum-targeting fluorescent probe for the imaging of endogenous H2S in live cells, *Spectrochimica Acta Part A: Molecular and Biomolecular Spectroscopy* (2020), https://doi.org/10.1016/j.saa.2020.118578

A highly sensitive endoplasmic reticulum-targeting fluorescent probe for the imaging of endogenous H_2S in live cells

Lei Zhou[a], Zhi-Qiang Cheng[a], Ning Li[a], Yong-Xi Ge[a], Hong-Xu Xie[a], Kongkai Zhu[b], Aiqin Zhou[c], Juan Zhang*[,a], Kai-Ming Wang*[,a], Cheng-Shi Jiang*[,a]

[a] *School of Biological Science and Technology, University of Jinan, Jinan 250022, China*

[b] *College of Chemistry and Molecular Engineering, Qingdao University of Science and Technology, Qingdao, 266042, China*

[c] *Collage of Horticulture, Qingdao Agricultural University, Qingdao, 266109, China*

*Corresponding author

E-mail addresses: bio_zhangj@ujn.edu.cn (J. Zhang); bio_wangkm@ujn.edu.cn (K.-M. Wang); jiangchengshi-20@163.com (C.-S. Jiang)

Tel/Fax: 0086-531-89736799

ABSTRACT

Hydrogen sulfide (H_2S) as an important signaling biomolecule participates in a series of complex physiological and pathological processes. In situ and rapid detection of H_2S levels in endoplasmic reticulum (ER) is of great importance for the in-depth study of its virtual functional roles. However, the ER-targeting fluorescent probe for the detection of H_2S in live cells is still quite rare. Herein, a new ER-targeting fluorescent probe (**FER-H_2S**) for detecting H_2S in live cells was characterized in the present study. This probe **FER-H_2S** was built from the hybridization of three parts, including fluorescein-based skeleton, *p*-toluenesulfonamide as ER-specific group, and 2,4-nitrobenzene sulfonate as a response site for H_2S. The response mechanism of the probe **FER-H_2S** to H_2S is on the basis of the ring-opening and ring-closing processes in fluorescein moiety. Moreover, the probe **FER-H_2S** was successfully used for the imaging of exogenous and endogenous H_2S in ER of live cells

Keywords: Endoplasmic reticulum; Hydrogen sulfide; Fluorescent probe; Xanthene; Fluorescein

1. Introduction

Hydrogen sulfide (H_2S) is a critical signaling reactive biomolecule, and plays important roles in numerous biological processes in living system [1-3]. H_2S is generally produced from L-cysteine or homocysteine by the catalysis of the enzymes including cystathionine-β-synthase, cystathionine-γ-lyase and 3-mercapto-pyruvate sulfurtransferase in the organs including liver, heart and kidney [4-6]. Recently, emerging evidences reveal that H_2S is implicated in a great number of pathological processes, such as inflammation, vasodilation and nervous system [7-11]. Moreover, H_2S also plays important roles in the protection against cardiac ischemia-reperfusion [12]. Even so, the endogenous H_2S in abnormal level could result in numerous malignant diseases including Alzheimer's disease, heart disease, diabetes, and cardiovascular diseases [13-16]. Therefore, the real-time and in situ detection of H_2S level is highly important for the further study of its roles in numerous biological processes.

Endoplasmic reticulum (ER), as one of the vital organelles in nearly all the eukaryotic cells, performs numerous critical physiological functions in the biosynthesis of protein, lipid manufacture and metabolism, cellular Ca^{2+} concentration stabilization, and detoxification [17-21]. Recently, a great variety of studies suggest that H_2S plays critical roles in the modulation of ER functions. The decrease of H_2S level in ER affects the phosphorylation of tyrosine-619 in PERK, and reduces the activation of tyrosine-619 under ER stress [22]. H_2S can result in the apoptosis of the insulin-secreting β cells by the increase of ER stress through P38 MAPK activation [23]. In spite of the remarkable advances in the study of H_2S in ER, many virtual functional roles of H_2S in ER still remain unknown. Thereinto, one of the crucial obstacles is the lack of effective methods for the real-time and in situ detection of H_2S level in ER, which is naturally in urgent need to be overcome.

Up to date, many available methods, including methylene blue colorimetric, electrochemical and chromatographic analytic methods, have been developed for the detection of H_2S [24-28]. However, these are generally not suitable for real-time and in situ detecting H_2S levels in the sophisticated live systems. In comparison with these

traditional methods, fluorescence imaging by molecular probes has become a more powerful tool due to its significant advantages in simple operation, real-time and in situ detection [29-35]. To date, a great many of fluorescent H_2S probes have been constructed on the basis of the reducibility of H_2S and the nucleophilicity of HS^- [36-43]. However, to the best of our knowledge, ER-targeting fluorescence probes for H_2S are still quite rare [44,45]. Therefore, the development of the ER-targeting fluorescent H_2S probes is still in urgent need.

Herein, a new ER-targeting fluorescein-based fluorescent probe (**FER-H_2S**) (Fig. 1) was designed and synthesized for the detection of exogenous and endogenous H_2S in live cells. The probe **FER-H_2S** was smoothly constructed from three pivotal functional fragments, including fluorescein-based potential fluorophore, *p*-toluenesulfonamide as the ER-targeting moiety, and 2,4-nitrobenzenesulfonate as a sensing site for H_2S. Before interacting with H_2S, **FER-H_2S** showed nearly no fluorescence because of ring-closing form of the spirolactone in the fluorescein moiety. Once in response to H_2S, the 2,4-nitrobenzene sulfonate unit was cleaved off from **FER-H_2S**, and the ring-opening response product generated simultaneously was strongly emissive. More importantly, the imaging experiments demonstrated that **FER-H_2S** could be successfully applied to the detection of the exogenous and endogenous H_2S in ER of live cells.

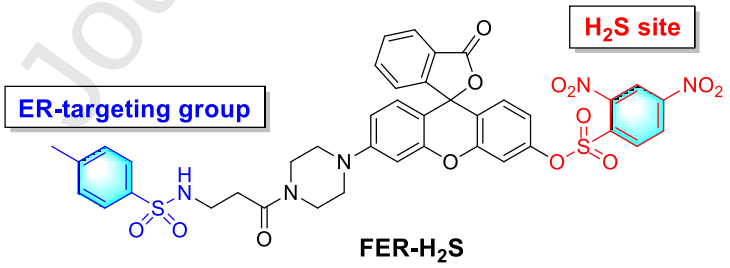

Fig. 1. The structure of **FER-H_2S**

2. Material and methods

2.1. Synthesis

Scheme 1 shows the synthetic route of **FER-H_2S**.

*2.1.1. Synthesis of **1***

To the mixture of β-alanine (446 mg, 5.0 mmol) in 4 mL distilled water was

added aqueous NaOH (2 M, 3.0 mL) and tosyl chloride (953 mg, 5.0 mmol). The reaction mixture was stirred at 35°C, and 2M aqueous NaOH was added to keep the pH value of the reaction system around 9. When the TLC indicated that the reaction was completed, the solution was filtered, and the organic phase was acidified to pH ~ 2 by addition of 0.5 M aqueous HCl at 0 °C. The obtained crystals were washed with cold water and dried to produce **1** as white solid (496 mg, 40.7%). ^{1}H NMR (600 MHz, DMSO-d_6) δ 12.27 (brs, 1H, CO_2H), 7.67 (d, J = 8.2 Hz, 2H), 7.58 (t, J = 5.8 Hz, 1H, NH), 7.40 (d, J = 8.2 Hz, 2H), 2.92–2.87 (m, 2H), 2.38 (s, 3H), 2.34 (t, J = 7.1 Hz, 2H). ^{13}C NMR (150 MHz, DMSO-d_6) δ 172.3, 142.7, 137.3, 129.7, 126.6, 38.6, 34.1, 21.0. ESI-MS: $[M+H]^+$ calcd for $C_{10}H_{14}NO_4S^+$ 244.0, found 244.0.

*2.1.2. Synthesis of **2***

To a solution of resorcinol (607 mg, 5.5 mmol) in 20 mL nitrobenzene was added phthalic anhydride (896 mg, 6.1 mmol) and $AlCl_3$ (2.2 g, 16.5 mmol). The solution was stirred overnight, and then poured into a mixed solution of hexanes (20.0 mL) and aqueous HCl (35.0 mL 0.5 M) for 2 h. The formed yellow precipitate was crystallized from EtOAc/PE to produce **2** as yellow solid (1.2 g, 85.0%). ^{1}H NMR (600 MHz, DMSO-d_6) δ 13.16 (brs, 1H, CO_2H), 12.23 (s, 1H), 10.72 (s, 1H), 7.99 (d, J = 7.5 Hz, 1H), 7.71 (td, J = 7.7, 7.5 Hz, 1H), 7.64 (dd, J = 7.7, 7.3 Hz, 1H), 7.42 (d, J = 7.3 Hz, 1H), 6.91 (d, J = 8.8 Hz, 1H), 6.32 (d, J = 2.2 Hz, 1H), 6.28 (dd, J = 8.8, 2.2 Hz, 1H). ^{13}C NMR (150 MHz, DMSO-d_6) δ 200.5, 166.7, 165.0, 164.4, 140.0, 134.7, 132.3, 130.0, 129.7, 129.4, 127.4, 113.2, 108.3, 102.5.

*2.1.3. Synthesis of **3***

A mixture of 3-aminophenol (655 mg, 6.0 mmol), diethylene glycolmonomethyl ether (3 mL), and bis(2-chloroethyl) aminehydrochloride (1.1 g, 6.0 mmol) was heated at 150 °C for 12 h in dry N_2 atmosphere. Then the mixture was cooled to room temperature, and poured into MeOH (5.0 mL) followed by addition of Et_2O (150.0 mL). The generate precipitate was washed with Et_2O to give compound **3** as brown solid (662 mg, 62.0%). ^{1}H NMR (600 MHz, DMSO-d_6) δ 9.11 (brs, 1H, CO_2H), 6.96 (dd, J = 8.1, 8.1 Hz, 1H), 6.34 (dd, J = 8.1, 2.1 Hz, 1H), 6.27 (dd, J = 2.2, 2.1 Hz, 1H), 6.18 (dd, J = 8.1, 2.2 Hz, 1H), 2.98–2.93 (m, 4H), 2.82–2.77 (m, 4H). ^{13}C NMR (150

MHz, DMSO-d_6) δ 158.1, 153.1, 129.4, 106.5, 106.0, 102.3, 49.3, 45.6. ESI-MS: $[M+H]^+$ calcd for $C_{10}H_{15}N_2O^+$ 179.1, found 179.0.

*2.1.4. Synthesis of **4***

Compound **2** (1.1 g, 4.4 mmol) was dissolved in CF_3CO_2H (15 mL), and then compound **3** (659 mg, 3.7 mmol) was added. The mixture was heated to reflux. After 36 h, the solution was concentrated, and the residues was purified by flash column chromatography using CH_3OH:DCM=1:6 to produce red solid **4** (800 mg, 54.0%). ^{1}H NMR (600 MHz, DMSO-d_6) δ 10.20 (brs, 1H, CO_2H), 8.00 (d, J = 7.4 Hz, 1H), 7.79 (dd, J = 7.4, 7.2 Hz, 1H), 7.72 (dd, J = 7.4, 7.2 Hz, 1H), 7.25 (d, J = 7.4 Hz, 1H), 6.91 (s, 1H), 6.77 (d, J = 8.0 Hz, 1H), 6.70 (s, 1H), 6.59 (d, J = 9.3 Hz,1H), 6.57–6.54 (m, 2H); 3.47 (brs, 4H), 3.24–3.17 (m, 5H). ^{13}C NMR (150 MHz, DMSO-d_6) δ 168.7, 159.6, 158.3, 158.2, 151.9, 151.8, 151.6, 135.6, 130.1, 129.98, 129.1, 128.6, 126.2, 124.7, 124.0, 112.1, 109.6, 109.4, 103.1, 102.0, 44.6, 42.4.

*2.1.5. Synthesis of **5***

Compound **1** (486 mg, 2.0 mmol), HATU (912 mg, 2.4 mmol), and DIEA (505 μL, 4.0 mmol) were successively added to a solution of compound **4** (800 mg, 2.0 mmol) in 25 mL of DCM/DMF (v/v, 5:1). The mixture was stirred for 12 h at room temperature, and then extracted using with mixed solution of DCM (30 mL) with water (30 mL). The organic phase was dried over Na_2SO_4, and then concentrated. The resulting restudies was subjected to flash column chromatography using CH_3OH/DCM (1/20, v/v) as the eluent to obtain compound **5** as a dark red solid (1.0 g, 81.0%).^{1}H NMR (600 MHz, $CDCl_3$) δ 8.23 (dd, J = 8.9, 0.9 Hz, 1H), 7.73 (ddd, J = 7.7, 7.5, 0.9 Hz, 1H), 7.75 (d, J = 8.2 Hz, 2H),7.66 (ddd, J = 8.0, 7.5, 1.0 Hz, 1H), 7.33–7.29 (m, 3H), 6.85 (d, J = 9.0 Hz, 1H), 6.83–6.80 (m, 2H), 6.67 (dd, J = 8.9, 2.1 Hz, 1H), 6.52 (dd, J = 8.9, 1.8 Hz, 1H), 6.44 (d, J = 1.4 Hz, 1H), 5.47 (t, J = 6.6 Hz, 1H, NH), 3.76 (t, J =5.1 Hz, 2H), 3.59 (t, J =5.4 Hz, 2H), 3.47–3.41 (m, 4H), 3.26–3.21 (m, 2H), 2.62 (t, J = 5.6 Hz, 2H), 2.42 (s, 3H). ^{13}C NMR (150 MHz, $CDCl_3$) δ 169.9, 165.9, 159.1, 154.7, 153.8, 143.6, 137.2, 134.8, 132.7, 131.2, 130.7, 130.5, 130.3, 130.1, 130.0, 129.9, 129.7, 129.4, 129.1, 127.1, 116.9, 113.3, 111.7, 105.8, 100.4, 52.5, 47.0, 44.6, 41.0, 39.2, 33.3, 21.7. ESI-MS *m/z* 626.0 $[M+H]^+$. HR-ESIMS:

$[M+H]^+$ calcd for $C_{34}H_{32}N_3O_7S^+$ 626.1955, found 626.1950.

*2.1.6. Synthesis of the probe **FER-H$_2$S***

To a solution of 2,4-dinitrobenzenesulfonyl chloride (89 mg, 0.6 mmol) in dry DCM (5.0 mL) was added compound **5** (74.5 mg, 0.12 mmol), and Et_3N (151 μL). The mixture was stirred at 0°C for 0.5 h, and then at room temperature for 12 h. The solution was concentrated to obtain a crude material, which was extracted with DCM/H_2O. The organic phase was dried over Na_2SO_4, and concentrated. The obtained residues was purified on silica gel column using CH_3OH/DCM (1/20, v/v) to yield **FER-H$_2$S** as a yellow solid (50 mg, 49.1%). ^{1}H NMR (600 MHz, $CDCl_3$) δ 8.66 (d, J = 2.1 Hz, 1H), 8.52 (dd, J = 8.7, 2.1 Hz, 1H), 8.25 (d, J = 8.7 Hz, 1H), 8.02 (d, J = 7.7 Hz, 1H), 7.74 (d, J = 7.6 Hz, 2H), 7.69 (dd, J = 7.5, 7.1 Hz, 1H), 7.64 (dd, J = 7.7, 7.1 Hz, 1H), 7.30 (d, J = 7.6 Hz, 2H), 7.18 (d, J = 2.2 Hz, 1H), 7.15 (d, J = 7.5 Hz, 1H), 6.87 (dd, J = 8.9, 2.1 Hz, 1H), 6.79 (d, J = 8.9 Hz, 1H), 6.67–6.63 (m, 2H), 6.60 (dd, J = 8.7, 2.4 Hz, 1H), 5.52 (t, J = 6.1 Hz, 1H, NH), 3.72 (t, J = 4.5 Hz, 2H), 3.54 (t, J = 4.4 Hz, 2H), 3.25–3.19 (m, 6H), 2.59 (t, J = 5.3 Hz, 2H), 2.40 (s, 3H). ^{13}C NMR (150 MHz, $CDCl_3$) δ 169.7, 169.2, 152.6, 152.6, 152.3, 152.0, 151.2, 149.5, 149.1, 143.5, 137.2, 135.5, 134.2, 133.4, 130.3, 130.2, 129.9, 129.0, 127.1, 126.8, 126.5, 125.4, 124.0, 120.6, 119.7, 117.2, 112.8, 111.1, 109.2, 102.4, 82.1, 48.2, 48.0, 44.8, 41.2, 39.2, 33.1, 21.6. ESI-MS *m/z* 856.0 $[M+H]^+$. HR-ESIMS: $[M+H]^+$ calcd for $C_{40}H_{34}N_5O_{13}S_2^+$ 856.1589, found 856.1599.

2.2. Fluorescence imaging of H2S in live cells

HepG2 cells were incubated in Eagle medium (10% fetal bovine serum and 1% antibiotic) under the environment with 5% CO_2 and 95% air at 37 °C. Subsequently, the HepG2 cells were transferred to glass-bottom culture dishes and then cultured overnight. All the fluorescent images in this work were acquired using a Nikon A1R confocal microscope.

For the imaging of the exogenous H_2S: HepG2 cells were pre-incubated with 5 μM **FER-H$_2$S** for 30 min and then washed by PBS buffer three times. Subsequently, the HepG2 cells were incubated with 100 μM or 200 μM Na_2S in PBS solution for another 30 min.

For the colocalization experiment of the probe **FER-H_2S** in live cells: After the pre-treatment of the HepG2 cells with 5 μM **FER-H_2S** for 30 min and 100 μM Na_2S in PBS solution for another 30 min, the HepG2 cells were stained with 1 μM ER-Tracker (a commercial ER tracker) for 5 min.

For the imaging of the endogenous H_2S: HepG2 cells were treated with 1 mM DL-propargylglycine (PAG) for 1 h, and then washed with PBS three times. Then, these cells were further stained with 5 μM **FER-H_2S** for 30 min. Finally, 200 μM Na_2S in PBS solution was added and the cells were incubated for another 30 min.

3. Results and discussion

*3.1. Design and synthesis of **FER-H_2S***

Fluorescein is well-known as an excellent and versatile fluorescent dye because of its high-profile physicochemical advantages, such as the brilliant photostability and the excellent fluorescence quantum yield. Meanwhile, the fluorescence property of the fluorescein could be conveniently controlled by regulating the ring opening/closing form of the fluorescein moiety in different response environments. Literature survey indicated that *p*-toluenesulfonamide could serve as an ER-specific unit, and thus it was embedded into the fluorescein moiety to endow the hybrid molecule with ER-targeting property. Besides, 2,4-nitrobenzenesulfonate could function as an excellent response site for H_2S. With these considerations in mind, the above-mentioned three fragments were fused into one molecule to construct a new ER-targeting fluorescein-based fluorescent probe (**FER-H_2S**), which can be employed for the real-time detection of H_2S in live cells.

The synthesis of the probe **FER-H_2S** was shown in Scheme 1. Briefly, treatment of β-alanine with tosyl chloride afforded **1**. Compounds **2** and **3** could be easily obtained from the starting materials, resorcinol/phthalic anhydride and 3-aminophenol/bis(2-chloroethyl) aminehydrochloride, respectively. The hybridization of **2** and **3** provided the fluorescein block **4**, which was then reacted with **1** to yield the key intermediate **5**. The target compound **FER-H_2S** was achieved through the esterification reaction of **5** and 2,4-dinitrobenzenesulfonyl chloride in the presence of Et_3N. The structures of these synthetic compounds were confirmed

by ^{1}H NMR, ^{13}C NMR and MS data (ESI†).

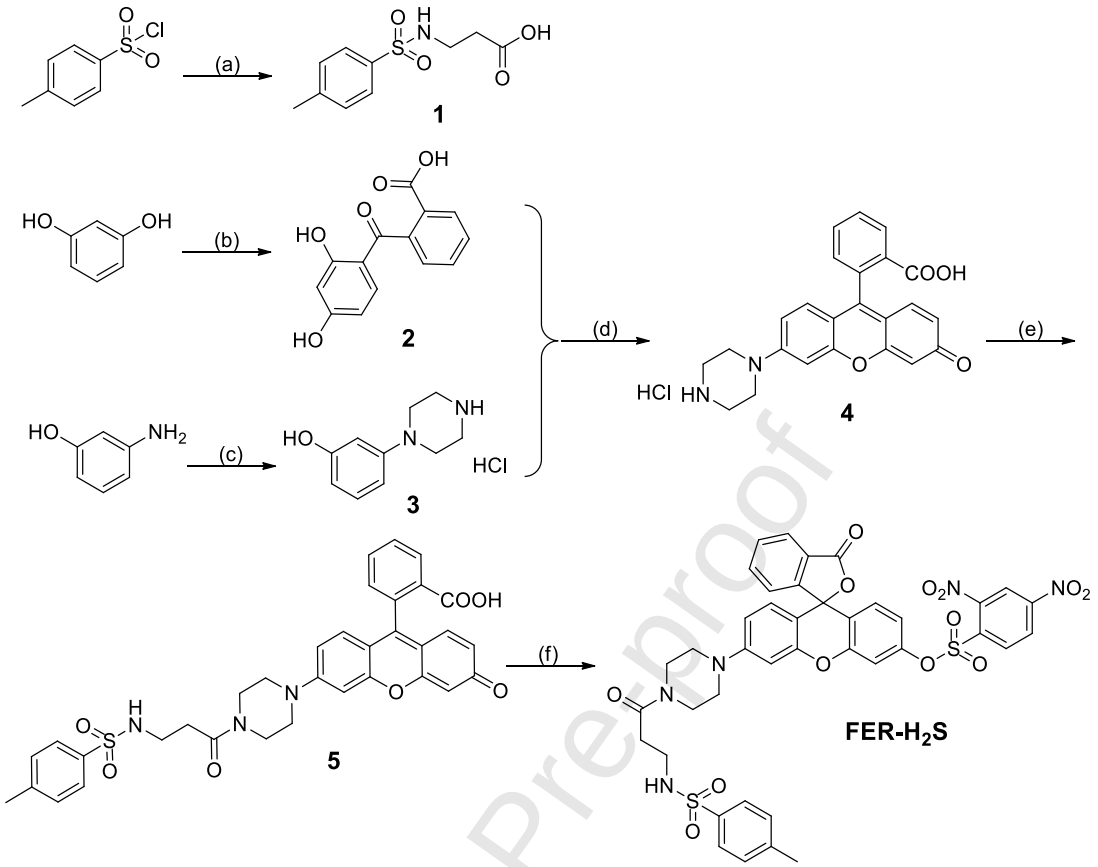

Scheme 1 Synthesis route of the probe **FER-H$_2$S**. (a) β-alanine, tosyl chloride, aqueous NaOH, r.t., overnight; (b) pathalic anhydride, $AlCl_3$, nitrobenzene, r.t., overnight; (c) bis(2-chloroethyl) aminehydrochloride, diethylene glycolmonomethyl ether, 150°C, 12 h; (d) CF_3CO_2H, reflux, 36 h; (e) **1**, HATU, DIEA, DCM/DMF (5:1), r.t., 12 h; (f) 2,4-dinitrobenzenesulfonyl chloride, Et_3N, DCM, r.t., 12 h.

*3.2. Optical response of **FER-H$_2$S** to H$_2$S*

Initially, the absorption and fluorescence spectra of **FER-H$_2$S** in the absence and presence of Na_2S were tested to assess the optical response of **FER-H$_2$S** to H_2S. In PBS buffer (20 mM, pH = 7.4) containing 10% EtOH, the probe **FER-H$_2$S** displayed nearly no obvious absorption in the visible region (Fig. S1, ESI†). After the treatment of the probe **FER-H$_2$S** with Na_2S at different concentrations, the absorption peak at 512 nm appeared and showed continuous increase with the increase of Na_2S concentrations, suggesting that the reaction between **FER-H$_2$S** and Na_2S occurs. **FER-H$_2$S** was nearly no emissive with the extremely low fluorescence quantum yield

(Φ < 0.0001) under excitation at 500 nm, due to the ring closing form of the xanthene moiety (Fig. 2A). When Na_2S was introduced into the solution of the probe **FER-H_2S**, a significant enhancement in the emission at 556 nm was observed clearly (Fig. 2A). The fluorescence intensity at 556 nm increased by about 100-fold after the response of **FER-H_2S** to 600 μM Na_2S. Meanwhile, the fluorescence intensity at 556 nm showed a desirable linear relationship with Na_2S in the concentration of 0-20 μM, and the calculated detection limit was 0. 081 μM (Fig. 2B). Furthermore, the time-dependent fluorescence spectra of 5 μM **FER-H_2S** to 100 μM Na_2S were then conducted to explore sensitivity of **FER-H_2S** to H_2S. The fluorescence intensity at 556 nm successively increased with time, and the fluorescence intensity at 556 nm could reach the plateau within 8 min (Fig. 2C and 2D). Taken together, **FER-H_2S** could be potentially employed as a sensitive fluorescent probe for the imaging of H_2S in live systems.

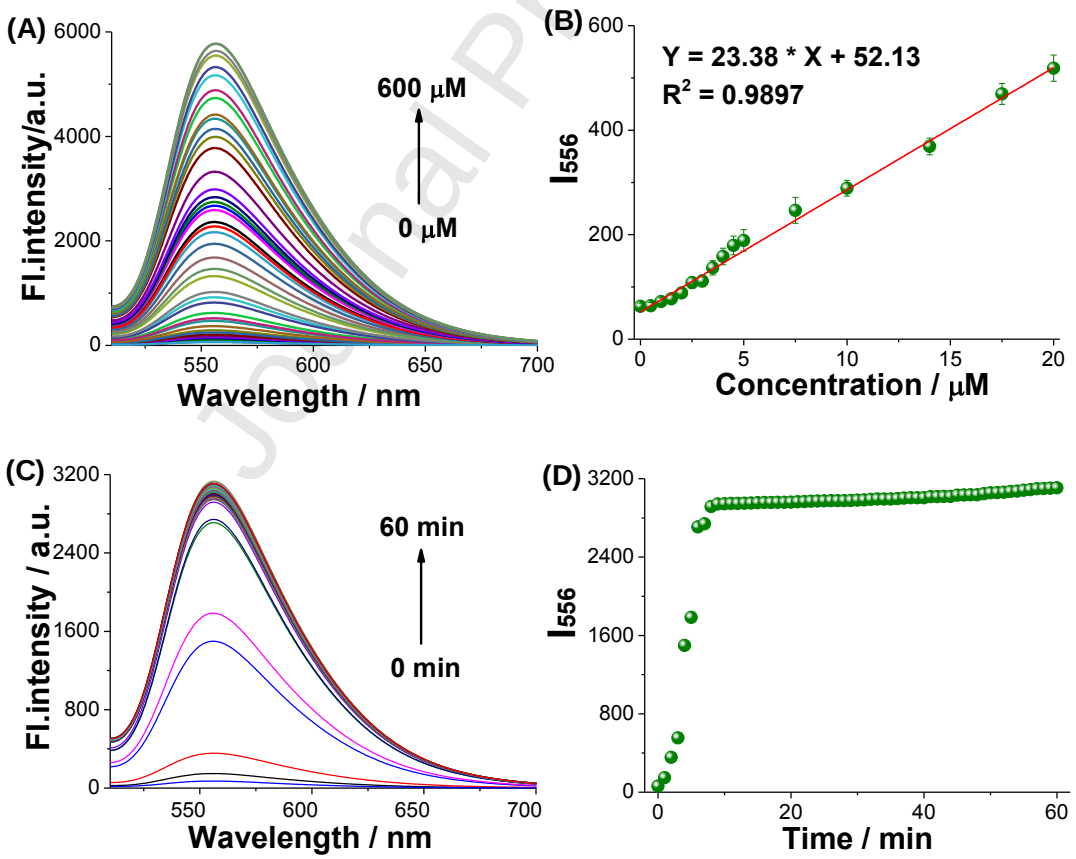

Fig. 2. (A) Fluorescence spectra of 5 μM **FER-H_2S** upon the addition of 0-600 μM Na_2S in PBS buffer (10% EtOH, pH = 7.4) under excitation at 500 nm. (B) Linearity

between the fluorescence intensity at 556 nm and Na_2S concentration in the range of 0 -20 μM. (C) Time-dependent fluorescence spectra of 5 μM **FER-H_2S** in the presence of 100 μM Na_2S under excitation at 500 nm in PBS (10% EtOH, pH = 7.4). (D) Fluorescence intensity at 556 nm as a function of time.

To explore the sensing mechanism of **FER-H_2S** to H_2S, the HRMS and HPLC tests were performed. HRMS data suggested that a peak at 626.1958 (Fig. S2, ESI†) ascribed to compound **5** (Cald. $[M+H]^+$ = 626.1955) can be found apparently after the reaction of **FER-H_2S** with Na_2S by the cleavage of 2,4-nitrobenzene sulfonate unit. Meanwhile, the HPLC data further suggested that the response product was the compound **5** after the treatment of **FER-H_2S** with Na_2S (Fig. S3, ESI†). Namely, the sensing mechanism of **FER-H_2S** to H_2S is on the basis of the cleavage of 2,4-nitrobenzene sulfonate unit (Scheme 2).

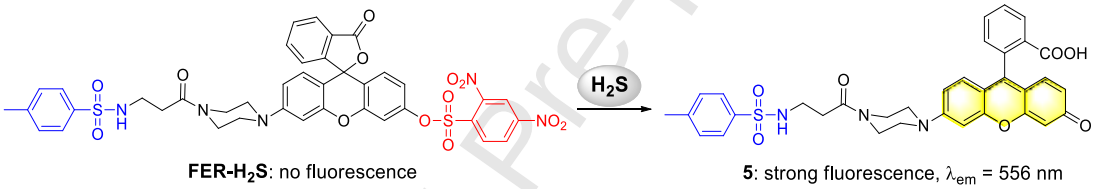

Scheme 2 Proposed response mechanism of **FER-H_2S** to H_2S.

*3.3. Selectivity of **FER-H_2S** towards H_2S*

To assess the selectivity of **FER-H_2S** to H_2S, the fluorescence spectra of **FER-H_2S** in the presence of a great variety of competing analytes such as various ions (Al^{3+}, Ca^{2+}, Zn^{2+}, F^-, I^-, SO_3^{2-}), biothiols (Cys, GSH, Hcy), ROS (H_2O_2, ClO^-, etc) and other biological species were conducted. As shown in the Fig. 3, the fluorescence intensity at 556 nm obviously increased after the reaction with Na_2S, whereas the other species lead to nearly no fluorescence response. These results suggest that **FER-H_2S** shows high selectivity to H_2S in comparison with other competing analytes and could be employed as a specific probe for the detection of H_2S in biological systems.

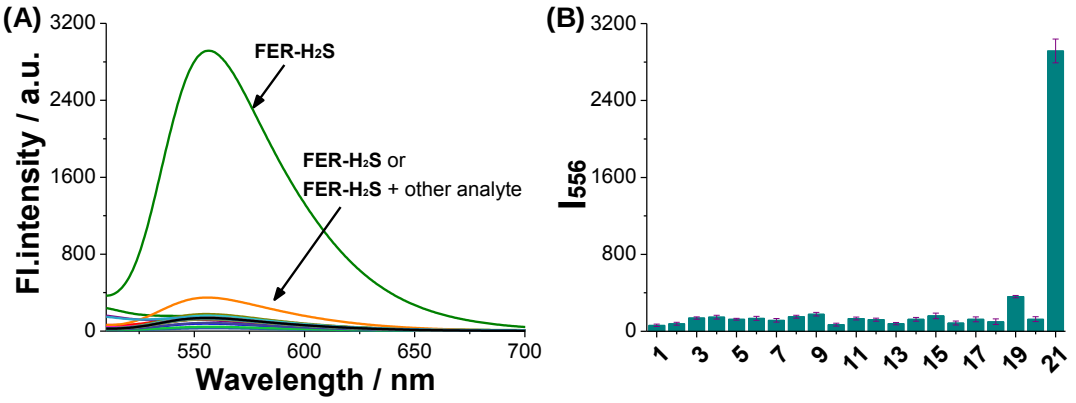

Fig. 3. Fluorescence spectra (A) and fluorescence intensity at 556 nm (B) of 5 μM **FER-H_2S** in the presence of various species in PBS buffer (10% EtOH, pH = 7.4) under excitation at 500 nm. 1, blank; 2, KI; 3, $CaCl_2$; 4, $FeSO_4$; 5, Cys; 6, $CoCl_2$; 7, $MgCl_2$; 8, NaBr; 9, NaF; 10, $CuSO_4$; 11, GSH; 12, H_2O_2; 13, TBHP; 14, DBTP; 15, Hcy; 16, $ZnCl_2$; 17,VC; 18, $NaNO_2$; 19, NaClO; 20, Na_2SO_3; 21,Na_2S. Concentration: GSH, 10 mM; other analytes, 100 μM.

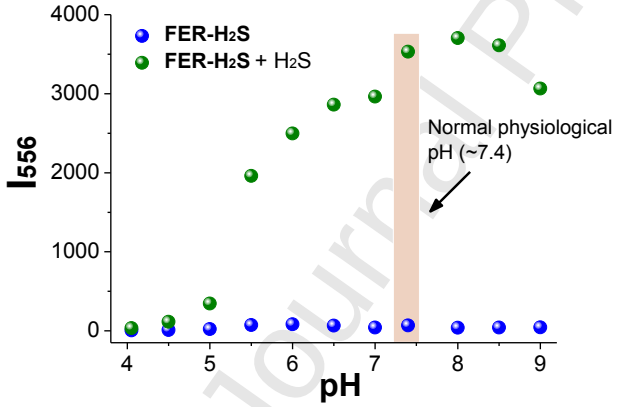

Fig. 4. The fluorescence responses of 5 μM **FER-H_2S** at 556 nm in the absence and presence of 100 μM Na_2S at different pH values.

The pH impact on the fluorescence spectra of **FER-H_2S** treated without or with Na_2S was then investigated to examine if **FER-H_2S** could work efficiently under physiological conditions. Before the reaction with Na_2S, the fluorescence spectra of **FER-H_2S** showed that the fluorescence was very weak in the pH range 4.0-9.0, suggesting that **FER-H_2S** exhibited desirable stability to different pH circumstance. After the addition of Na_2S to the solution of the probe, **FER-H_2S** could show desirable response to Na_2S in the pH range 5.5-9.0 (Fig. 4 and Fig. S4, ESI†). Taking

into consideration of the normal physiological pH at about 7.4, **FER-H_2S** could serve as an available probe for monitoring H_2S in live systems.

3.4. Fluorescence imaging in live cells

The feasibility of **FER-H_2S** to image cellular H_2S was subsequently investigated using live HepG2 cells. Firstly, MTT assay was performed to test the cytotoxicity of **FER-H_2S** with different concentrations to live HepG2 cells (Fig. S5, ESI†). The MTT data showed that **FER-H_2S** possessed no significant cytotoxicity below the concentration of 20 μM and was available for the fluorescence imaging of cellular H_2S. As depicted in Fig. 5, when the live cells were firstly stained with 5 μM **FER-H_2S** for 30 min, there was very weak fluorescence in green channel. However, after the further treatment of the HepG2 cells with 100 μM or 200 μM Na_2S, the strong fluorescence in green channel appeared clearly, and the fluorescence intensity obviously enhanced with the Na_2S level changed from 100 μM to 200 μM. It suggests that the probe **FER-H_2S** could be employed to image exogenous H_2S in live cells.

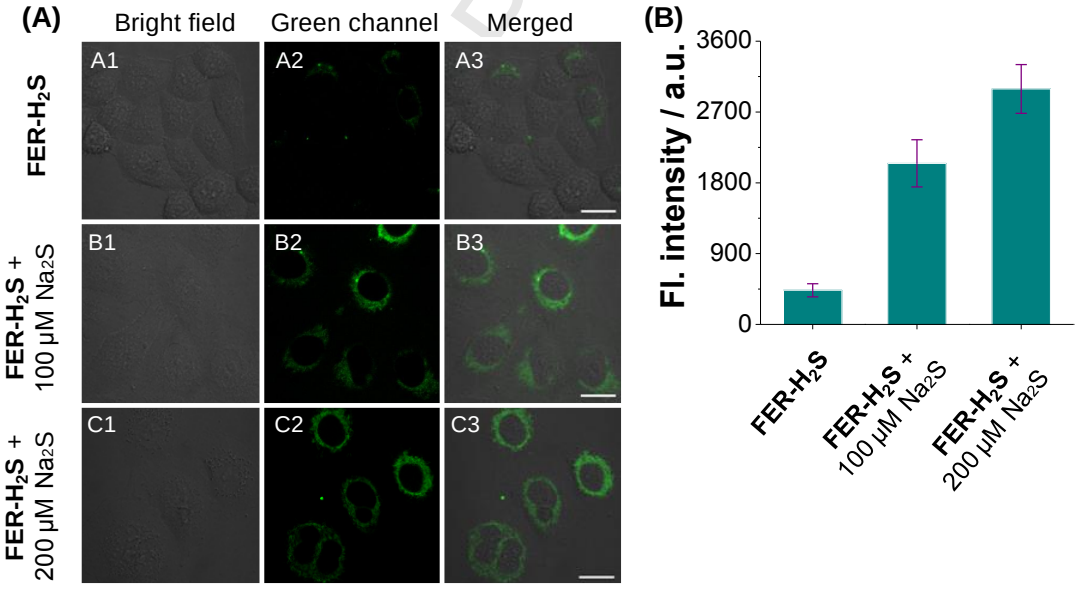

Fig. 5. (A) A1-A3: Images of HepG2 cells treated with 5 μM **FER-H_2S** for 30 min; B1-B3: Images of HepG2 cells treated with 5 μM **FER-H_2S** for 30 min and the treated with 100 μM Na_2S for another 30 min; C1-C3: Images of HepG2 cells treated with 5 μM **FER-H_2S** for 30 min and the treated with 200 μM Na_2S for another 30 min. λ_{em} = 500-550 nm, λ_{ex} = 488 nm. Scale bar = 20 μm. (B) Quantified fluorescence intensity of a single cell in Green channel analyzed by ImageJ software.

We then assessed the feasibility of **FER-H_2S** to selectively visualize H_2S in ER of live cells. The colocalization experiments were performed to check the main distribution of **FER-H_2S** at subcellular level by using live HepG2 cells and a commercial ER tracker. The cells were firstly stained with 5 μM **FER-H_2S** for 30 min and treated with 100 μM Na_2S for 30 min, and then incubated with 1 μM ER-Tracker for 5 min. As depicted in Fig. 6, the fluorescence in green channel was generated from the response **FER-H_2S** to cellular Na_2S, and displayed prominent overlap with the fluorescence in blue green that produced from ER-tracker. The calculated Pearson's colocalization coeffcient (R) value of the fluorescence in blue and green channels was 0.93. Therefore, the probe **FER-H_2S** was mainly distributed in ER and can be employed as an ER-specific probe.

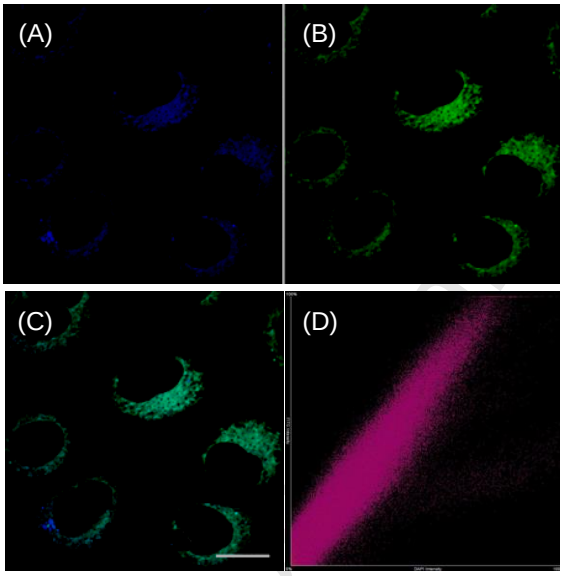

Fig. 6. Fluorescence images of HepG2 cells treated with 5 μM **FER-H_2S** for 30 min and the treated with 100 μM Na_2S for another 30 min, and then treated with 1 μM ER-tracker for 5 min. (A) Fluorescence image of ER-Tracker Blue collected at 425-475 nm at 405 nm excitation. (B) Fluorescence image of **FER-H_2S** collected at 500-550 nm at 488 nm excitation. (C) Merged image of (A) and (B). (D) Correlation plot of the fluorescence intensity in (A) and (B). Scale bar = 20 μm.

Finally, the capability of **FER-H_2S** to detect endogenous H_2S was investigated. When the HepG2 cells were only stained with 5 μM **FER-H_2S** for 30 min, the cells showed very weak fluorescence under excitation at 488 nm. DL-propargylglycine

(PAG), is an efficient inhibitor for H_2S, which can reduce the endogenous H_2S levels in live systems by lowering the activity of L-cysteine desulfhydrase (LCD) and D-cysteine desulfhydrase (DCD) [46,47]. When the HepG2 cells were stimulated by 1 mM PAG for 1 h and subsequently treated with 5 μM **FER-H_2S** for another 30 min, nearly no fluorescence could be observed (Fig. 7). It indicates that the endogenous H2S level in live cells decreases under the stimulation of PAG. Meanwhile, the fluorescence intensity in green channel of the cells treated with 1 mM PAG and 5 μM **FER-H_2S** was significantly enhanced after the further addition of 200 μM Na_2S, indicating that the probe **FER-H_2S** shows fluorescence response to the exogenous H_2S (Fig. 7). Therefore, the probe **FER-H_2S** could be applied to detect endogenous H_2S in ER of live cells.

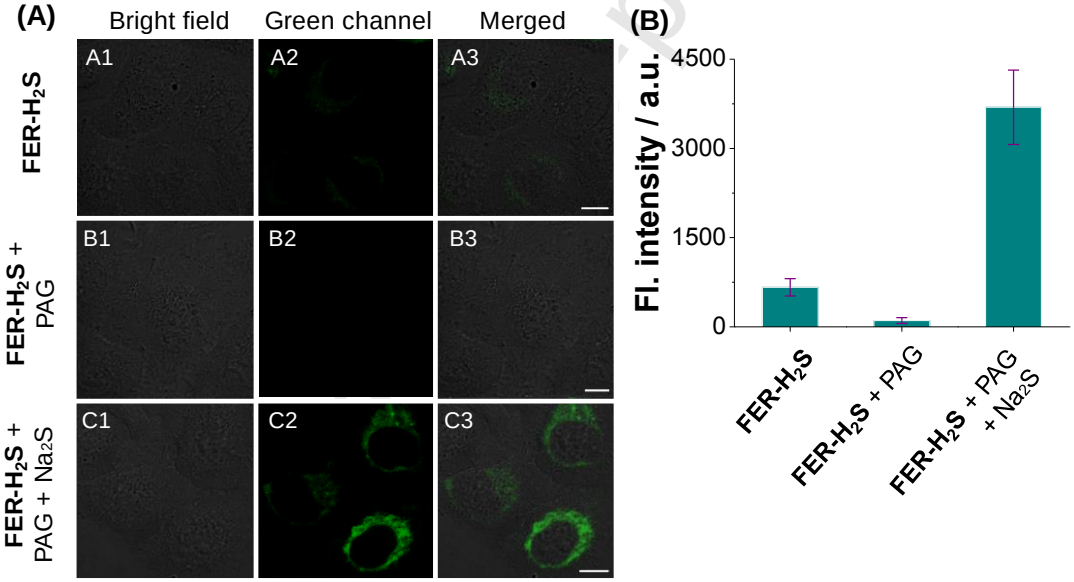

Fig. 7. (A) Fluorescence images of HepG2 cells treated with 5 μM **FER-H_2S** for 30 min (A1-A3). HepG2 cells were pre-treated with 1 mM PAG for 1 h and then incubated with 5 μM **FER-H_2S** for 30 min (B1-B3), then incubated with 200 μM Na_2S for 30 min (C1-C3), λ_{em} = 500-550 nm, λ_{ex} = 488 nm. Scale bar = 20 μm. (B) Quantified fluorescence intensity of a single cell in Green channel analyzed by ImageJ software.

4. Conclusions

In conclusion, a new fluorescent probe (**FER-H_2S**) was constructed for the detection of H_2S in ER. This probe **FER-H_2S** was built from the hybridization of

three parts, including fluorescein-based skeleton, *p*-toluenesulfonamide as ER-specific group and 2,4-nitrobenzene sulfonate as a response site for H_2S. The response mechanism of the probe **FER-H_2S** to H_2S is on the basis of the ring opening/clsosing of the xanthene in fluorescein moiety. Moreover, the probe **FER-H_2S** was successfully used for the imaging of exogenous and endogenous H_2S in ER of live cells.

Declaration of competing interest

The authors declare that they have no known competing financial interests or personal relationships that could have appeared to influence the work reported in this paper

Acknowledgements

This work was financially supported by the Agricultural Variety Improvement Project of Shandong Province of China [No. 2019LZGC007], National Natural Science Foundation of China [Nos. 21672082, 81603215], Natural Science Foundation of Shandong Province [Nos. ZR2019YQ31, ZR2017BC101], Doctoral Fund Project of University of Jinan [No. 301/160100394], Shandong Talents Team Cultivation Plan of University Preponderant Discipline [No. 10027].

References

[1] R. Wang, Hydrogen sulfide: the third gasotransmitter in biology and medicine, Antioxid. Redox Signal, 12 (9) (2010) 1061−1064.

[2] H.M. Kim, B.R. Cho, Small-molecule two-photon probes for bioimaging applications, Chem. Rev. 115 (11) (2015) 5014−5055.

[3] L. Li, P. Rose, P.K. Moore, Hydrogen sulfide and cell signaling, Annu. Rev. Pharmacol. Toxicol. 51 (2011) 169–187.

[4] S. Singh, D. Padovani, R.A. Leslie, T. Chiku, R.J. Banerjee, Relative contributions of cystathionine beta-synthase and gamma-cystathionase to H_2S biogenesis via alternative trans-sulfuration reaction, J. Biol. Chem. 284 (33)

(2009) 22457−22466.

[5] N. Shibuya, M. Tanaka, M. Yoshida, Y. Ogasawara, T. Togawa, K. Ishii, H. Kimura, 3-Mercaptopyruvate sulfurtransferase produces hydrogen sulfide and bound sulfane sulfur in the brain, Antioxid. Redox Signaling 11 (4) (2009) 703–714.

[6] J. Sarfraza, P. Ihalainena, A. Maattanena, T. Gulina, J. Koskelab, C.E. Wilen, A. Kilpelab, J. Peltonena, A printed H_2S sensor with electro-optical response, Sensors Actuat. B Chem. 191 (2014) 821–827.

[7] A. Papapetropoulos, A. Pyriochou, Z. Altaany, G. Yang, A. Marazioti, Z. Zhou, M. G. Jeschke, L.K. Branski, D.N. Herndon, R. Wang, C. Szabó, Hydrogen sulfide is an endogenous stimulator of angiogenesis, Proc. Natl. Acad. Sci. U.S.A. 106 (51) (2009) 21972−21977.

[8] L. Li, M. Bhatia, Y.Z. Zhu, Y.C. Zhu, R.D. Ramnath, Z.J. Wang, F.B. Mohammed, M. Whiteman, M. Salto-Tellez, P.K. Moore, Hydrogen sulfide is a novel mediator of lipopolysaccharide-induced inflammation in the mouse, FASEB J. 19 (9) (2005) 1196−1198.

[9] G.D. Yang, L.Y. Wu, B. Jiang, W. Yang, J.S. Qi, K. Cao, Q.H. Meng, A.K. Mustafa, W.T. Mu, S.M. Zhang, S.H. Snyder, R. Wang, H_2S as a physiologic vasorelaxant: hypertension in mice with deletion of cystathionine gamma-lyase, Science 322 (590) (2008) 587−590.

[10] M.L. Lo Faro, B. Fox, J.L. Whatmore, P.G. Winyard, M. Whiteman, Hydrogen sulfide and nitric oxide interactions in inflammation, Nitric Oxide 41 (2014) 38−47.

[11] L. Li, P. Rose, P. K. Moore, Hydrogen sulfide and cell signaling, Annu. Rev. Pharmacol. Toxicol. 51 (2011) 169-187.

[12] B.L. Predmore, K. Kondo, S. Bhushan , M.A. Zlatopolsky, A.L. King, J.P. Aragon, D.B. Grinsfelder, M.E. Condit, D.J. Lefer, The polysulfide diallyl trisulfide protects the ischemic myocardium by preservation of endogenous hydrogen sulfide and increasing nitric oxide bioavailability, Am. J. Physiol. Heart Circ. Physiol. 302 (11) (2012) H2410-H2418.

[13] P. Kamoun, M.C. Belardinelli, A. Chabli, K. Lallouchi, B. Chadefaux-Vekemans, Endogenous hydrogen sulfide overproduction in Down syndrome, Am. J. Med. Genet. A. 116A (3) (2003) 310−311.

[14] S. Fiorucci, E. Antonelli, A. Mencarelli, S. Orlandi, B. Renga, G. Rizzo, E. Distrutti, V. Shah, A. Morelli, The third gas: H_2S regulates perfusion pressure in both the isolated and perfused normal rat liver and in cirrhosis, Hepatology 42 (3) (2005) 539−548.

[15] K. Eto, T. Asada, K. Arima, T. Makifuchi, H. Kimura, Brain hydrogen sulfide is severely decreased in Alzheimer's disease, Biochem. Biophys. Res. Commun. 293 (5) (2002) 1485−1488.

[16] L. Wu, W. Yang, X. Jia, G. Yang, D. Duridanova, K. Cao, R. Wang, Pancreatic islet overproduction of H_2S and suppressed insulin release in Zucker diabetic rats, Lab. Invest. 89 (1) (2009) 59−67.

[17] P. Quinn, G. Griffiths, G. Warren, Density of newly synthesized plasma membrane proteins in intracellular membranes. I. Stereological studies, J. Cell Biol. 98 (6) (1984) 2142−2147.

[18] O. Baumann, B. Walz, Endoplasmic reticulum of animal cells and its organization into structural and functional domains, Int. Rev. Cytol. 205 (2001) 149−214.

[19] R. Sitia, I. Braakman, Quality control in the endoplasmic reticulum protein factory, Nature 426 (6968) (2003) 891−894.

[20] L. Ellgaard, A. Helenius, Quality control in the endoplasmic reticulum, Nat. Rev. Mol. Cell Biol. 4 (3) (2003) 181−191.

[21] A. Görlach, P. Klappa, T. Kietzmann, The endoplasmic reticulum: folding, calcium homeostasis, signaling, and redox control, Antioxid. Redox Signal. 8 (9-10) (2006) 1391−1418.

[22] N. Krishnan, C.X. Fu, D.J. Pappin, N.K. Tonks, H_2S-Induced sulfhydration of the phosphatase PTP1B and its role in the endoplasmic reticulum stress response, Sci. Signal. 4 (203) (2011) R86−R97.

[23] G.D. Yang, W. Yang, L.Y. Wu, R. Wang, H_2S, endoplasmic reticulum stress, and apoptosis of insulin-secreting beta cells, J. Biol. Chem. 282 (22) (2007)

16567−16576.

[24] J. Radfordknoery, G.A. Cutter, Determination of carbonyl sulfide and hydrogen sulfide species in natural waters using specialized collection procedures and gas chromatography with flame photometric detection, Anal. Chem. 65 (8) (1993) 976–982.

[25] T.W. Mitchell, J.C. Savage, D.H. Gould, High-performance liquid chromatography detection of sulfide in tissues from sulfide-treated mice, J. Appl. Toxicol. 13 (6) (1993) 389−394.

[26] V. Kuban, P.K. Dasgupta, J.N. Marx, Nitroprusside and methylene blue methods for silicone membrane differentiated flow injection determination of sulfide in water and wastewater, Anal. Chem. 64 (1) (1992) 36−43.

[27] M.N. Hughes, M.N. Centelles, K.P. Moore, Making and working with hydrogen sulfide: The chemistry and generation of hydrogen sulfide in vitro and its measurement in vivo: a review, Free Radic. Biol. Med. 47 (10) (2009) 1346−1353.

[28] T. Xu, N. Scafa, L.P. Xu, S. Zhou, K. Abdullah Al-Ghanem, S. Mahboob, B. Fugetsu, X. Zhang, Electrochemical hydrogen sulfide biosensors, Analyst 141 (4) (2016) 1185–1195.

[29] J.R. Lakowicz, Principles of Fluorescence Spectroscopy, Springer, New York, 3rd edn, 2006.

[30] H.S. Jung, P. Verwilst, W.Y. Kim, J.S. Kim, Fluorescent and colorimetric sensors for the detection of humidity or water content, Chem. Soc. Rev. 45 (5) (2016) 1242−1256.

[31] L. Zhang, S. Peng, J. Sun, R. Liu, S. Liu, J. Fang, A ratiometric fluorescent probe of methionine sulfoxide reductase with an improved response rate and emission wavelength, Chem. Commun. 55 (10) (2019) 1502−1505.

[32] A. Xu, Y. He, W. Ying, Endoplasmic Reticulum-Targeted Two-Photon Turn-On Fluorescent Probe for Nitroreductase in Tumor Cells and Tissues, Spectrochim Acta A Mol. Biomol. Spectrosc. 204 (2019) 770−776.

[33] Q. Xia, X. Wang, Y. Liu, Z. Shen, Z. Ge, H. Huang, X. Li, Y. Wang, An

Endoplasmic Reticulum-Targeted Two-Photon Fluorescent Probe for Bioimaging of HClO Generated During Sleep Deprivation, Spectrochim Acta A Mol. Biomol. Spectrosc. 229 (2020) 117992.

[34] H. Meng, X-Q. Huang, Y. Lin, D.-Y. Yang, Y.-J. Lv, X.-Q. Cao, G.-X. Zhang, J. Dong, S. L. Shen, A New Ratiometric Fluorescent Probe for Sensing Lysosomal HOCl Based on Fluorescence Resonance Energy Transfer Strategy, Spectrochim Acta A Mol. Biomol. Spectrosc. 223 (2019) 117355.

[35] X.-F. Zhang, T.-R. Wang, X.-Q. Cao, S.-L. Shen, A Near-Infrared Rhodamine-Based Lysosomal pH Probe and Its Application in Lysosomal pH Rise During Heat Shock, Spectrochim Acta A Mol. Biomol. Spectrosc. 227 (2020) 117761.

[36] V.S. Lin, W. Chen, M. Xian, C.J. Chang, Chemical probes for molecular imaging and detection of hydrogen sulfide and reactive sulfur species in biological systems, Chem. Soc. Rev. 44 (14) (2015) 4596–4618.

[37] A.C. Sedgwick, L. Wu, H.H. Han, S.D. Bull, X.P. He, T.D. James, J.L. Sessler, B.Z. Tang, H. Tian, J. Yoon, Excited-state intramolecular proton-transfer (ESIPT) based fluorescence sensors and imaging agents, Chem. Soc. Rev. 47 (23) (2018) 8842−8880.

[38] Y. Yue, F. Huo, F. Cheng, X. Zhu, T. Mafireyi, R.M. Strongin, C. Yin, Functional synthetic probes for selective targeting and multi-analyte detection and imaging, Chem. Soc. Rev. 48 (15) (2019) 4155–4177.

[39] J. Liu, Y.Q. Sun, J. Zhang, T. Yang, J. Cao, L. Zhang, W. Guo, A ratiometric fluorescent probe for biological signaling molecule H_2S: fast response and high selectivity, Chemistry 19 (15) (2013) 4717–4722.

[40] T. Cao, Z. Teng, D. Gong, J. Qian, W. Liu, K. Iqbal, W. Qin, H. Guo, A ratiometric fluorescent probe for detection of endogenous and exogenous hydrogen sulfide in living cells, Talanta 198 (2019) 185–192.

[41] M. Gao, F. Yu, H. Chen, L. Chen, Near-infrared fluorescent probe for imaging mitochondrial hydrogen polysulfides in living cells and in vivo, Anal. Chem. 87 (7) (2015) 3631–3638.

[42] N. Kang, S. Pei, C. Zhang, G. Zhang, Y. Zhou, L. Shi, W. Wang, S. Shuang, C. Dong, A Turn-On Fluorescence Probe for Hydrogen Sulfide in Absolute Aqueous Solution, Spectrochim Acta A Mol. Biomol. Spectrosc. 233 (2020) 118156.

[43] X. Lin, X. Lu, J. Zhou, H. Ren, X. Dong, W. Zhao, Z. Chen, Instantaneous Fluorescent Probe for the Specific Detection of H_2S, Spectrochim Acta A Mol. Biomol. Spectrosc. 213 (2019) 416–422.

[44] Y. Tang, A. Xu, Y. Ma, G. Xu, S. Gao, W. Lin, A turn-on endoplasmic reticulum-targeted two-photon fluorescent probe for hydrogen sulfide and bio-imaging applications in living cells, tissues, and zebrafish, Sci. Rep. 7 (1) (2017) 12944–12950.

[45] H. Zhang, J. Chen, H. Xiong, Y. Zhang, W. Chen, J. Sheng, X. Song, An endoplasmic reticulum-targetable fluorescent probe for highly selective detection of hydrogen sulfide, Org. Biomol. Chem. 17 (6) (2019) 1436–1441.

[46] H.M.S.Al Ubeed, R.B.H. Wills, M.C. Bowyer, J.B. Golding, Interaction of the hydrogen sulphide inhibitor, propargylglycine (PAG), with hydrogen sulphide on postharvest changes of the green leafy vegetable, pak choy, Postharvest Biol. Tec. 147 (2019) 54–58.

[47] W. Hua, F. Zheng, Y. Wang, Y. Wang, S. Fu, W. Wang, C. Xie, Y. Zhang, F. Gong, Inhibition of endogenous hydrogen sulfide production improves viral elimination in CVB3-infected myocardium in mice, Pediatr. Res., 85 (4) (2019) 533–538.

Credit author statement

Cheng-Shi Jiang directed the research, and reviewed the paper.

Juan Zhang and **Kai-Ming Wang** designed and performed the experiments, analyzed the data, and wrote the paper.

Lei Zhou performed the experiments and analyzed the data;

Zhi-Qiang Cheng, **Ning Li**, **Yong-Xi Ge**, **Hong-Xu Xie**, **Kongkai Zhu**, and **Aiqin Zhou** helped with the experiments and analyzed the data.

All the authors discussed the results and commented on the manuscript.

Declaration of interests

☒ The authors declare that they have no known competing financial interests or personal relationships that could have appeared to influence the work reported in this paper.

☐The authors declare the following financial interests/personal relationships which may be considered as potential competing interests:

Graphic abstract

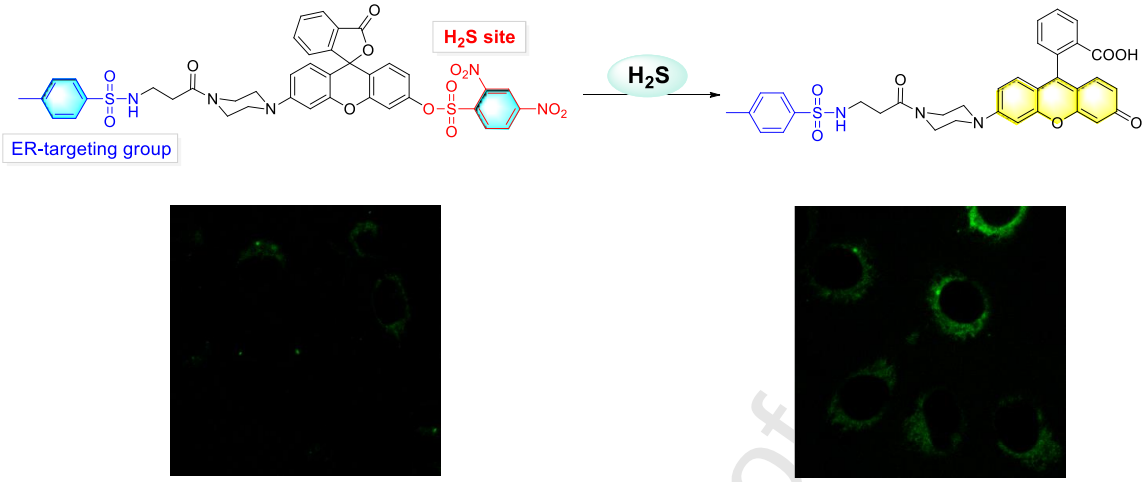

Highlight

1. A novel ER-targeting fluorescent probe (**FER-H_2S**) for H_2S was designed.
2. The probe **FER-H_2S** showed high sensitive and selective response to H_2S.
3. The probe **FER-H_2S** can be applied for the imaging of endogenous H_2S in live cells.